

with information about population structure from other such 'vagabond' fauna and flora, should continue to shed light on the vagaries of human evolution.

Christopher C. Austin

*Evolutionary Biology Unit,
South Australian Museum,
Adelaide 5000, Australia*

*Present address: Institute of Statistical Mathematics,
4-6-7 Minami-Azabu Minato-ku,
Tokyo 106-8569, Japan
e-mail: caustin@ism.ac.jp*

1. Diamond, J. M. *Nature* **336**, 307–308 (1988).
2. Terrell, J. *Antiquity* **62**, 642–657 (1988).
3. Clegg, J. B. *Lancet* **344**, 1070–1071 (1994).
4. Bellwood, P. S. in *The Colonization of the Pacific: Some Current Hypotheses* (eds Hill, A. V. S. & Serjeantson, S. W.) 1–59 (Oxford Univ. Press, 1989).
5. Kirch, P. V. & Hunt, R. L. *Radiocarbon* **30**, 161–169 (1988).
6. Pawley, A. & Green, R. *Ocean Ling.* **12**, 1–67 (1973).
7. Hagelberg, E. & Clegg, J. B. *Proc. R. Soc. Lond. B* **252**, 163–170 (1993).
8. Redd, A. J. *et al. Mol. Biol. Evol.* **12**, 604–615 (1995).
9. Martinson, J. J. in *Molecular Biology and Human Diversity* (eds Boyce, A. J. & Mascie-Taylor, C. G. N.) 171–195 (Cambridge Univ. Press, 1996).
10. Thorpe, R. S., McGregor, D. P., Cumming, A. M. & Jordan, W. C. *Evolution* **48**, 230–240 (1994).

The first true inorganic fullerenes?

Boron nitride and materials of composition MX_2 , where M is molybdenum or tungsten and X is sulphur or selenium, can form fullerene-like structures such as nested polyhedra or nanotubes^{1–3}. However, the analogy to the carbon fullerene family⁴ falls short because no small preferred structure akin to C_{60} (ref. 5) has been found. We have discovered nano-octahedra of MoS_2 of discrete sizes in soots that we prepared by laser ablation of pressed MoS_2 targets. These nano-octahedra are much larger than C_{60} structures, having edge lengths of about 4.0 and 5.0 nanometres, and may represent the first 'inorganic fullerenes'.

Targets were prepared by pressing 98% pure MoS_2 powder and ablated using a KrF pulsed excimer laser (8 Hz, 248 nm, ~300 mJ per pulse, ~20 ns per pulse, ~10 J cm⁻²) under flowing helium or argon (500–800 torr, ~90 cm³ min⁻¹). The beam was moved every 4 minutes during the 20-minute runs to strike fresh target material, with the chamber and target temperature ranging from 30 to 600 °C. The soot generated was collected, ultrasonicated in acetone, and applied to a grid for imaging by transmission electron microscopy (TEM).

Soot produced between 30 and 500 °C contained crystalline and amorphous MoS_2 fractions, as well as smaller rhomboidal, rectangular and hexagonal structures 3 to 5 nm long with two or three layers. The crystalline material included large sheets and tubes and a variety of nested polyhedra 15

to 35 nm long that were similar to those produced previously⁶. Above 550 °C, only crystalline folded sheets of MoS_2 were produced.

TEM stage-tilting experiments on 30 two- and three-layered structures showed that the small rhomboids, rectangles and hexagons were different projections of the same three-dimensional structure: an octahedron (Fig. 1a). The TEM image for a closed three-layer structure changes with tilts of 10° and 20° (Fig. 1b). The image at 0° is the projection expected for an octahedron orientated such that only two triangular faces are seen. When it is tilted, the projection changes, resulting in a nearly rectangular projection at 20°. Stick models depicting how an octahedron's projection changes with tilting are also shown in Fig. 1b. The model octahedron was orientated to project a match to the 0° image, and the model was then tilted with the same axis used in the TEM. Many other TEM tilt

sequences could also be generated with projections of a model octahedron. In some cases, slight movements of the particles on the TEM grid ruined the correlation, but individual images could still be represented by the projection of an octahedron.

The edge length of the octahedron may be calculated from TEM projections, assuming a regular octahedral structure. A histogram of edge lengths for 30 different structures is shown in Fig. 1c. Two pronounced peaks are seen at 12–13 and 16 times the *a* lattice constant (the Mo–Mo distance, 3.16 Å) of MoS_2 for two- and three-layer species, respectively. The spacing between the layers is about 0.6 nm, in good agreement with the interlayer spacing in bulk MoS_2 . The edge of the three-layer species is about four *a* lattice constants larger than that of the underlying two-layer structure, exactly the size required to maintain the bulk interlayer spacing.

Although the reasons for these specific sizes are not clear, a preference for two- and three-layer structures may be associated with the two- and three-layer polytypes⁷. The octahedral shape might be anticipated for a closed MoS_2 structure as the triangular faces share the symmetry of the trigonal Mo and S sublattices. Rounded corners and edges are also expected for MoS_2 sheets, which cannot be severely bent without strain. Energy-dispersive spectroscopy indicated a Mo:S ratio of about 1:2 with no detectable impurities. Satisfying such a ratio exactly is impossible in an octahedron, but several arrangements come close. For example, the Mo–S coordination could remain trigonal prismatic, as in the bulk form, with a given face being slightly rich or poor in sulphur. The structure at the vertices is unclear, but either a four-membered Mo ring³ or a single Mo atom might be stable (B. Parkinson, personal communication).

TEM measurements could be performed only on nano-octahedra that were separated from the agglomerates formed on the TEM grid. Consequently, we cannot yet estimate the density of nano-octahedra in the laser-generated soots. We are purifying these inorganic fullerenes so that we can ascertain their properties, and are also finding out whether similar cage structures can be made using other layered materials.

P. A. Parilla, A. C. Dillon, K. M. Jones, G. Riker, D. L. Schulz, D. S. Ginley, M. J. Heben

*National Renewable Energy Laboratory,
1617 Cole Boulevard, Golden,
Colorado 80401-3393, USA*

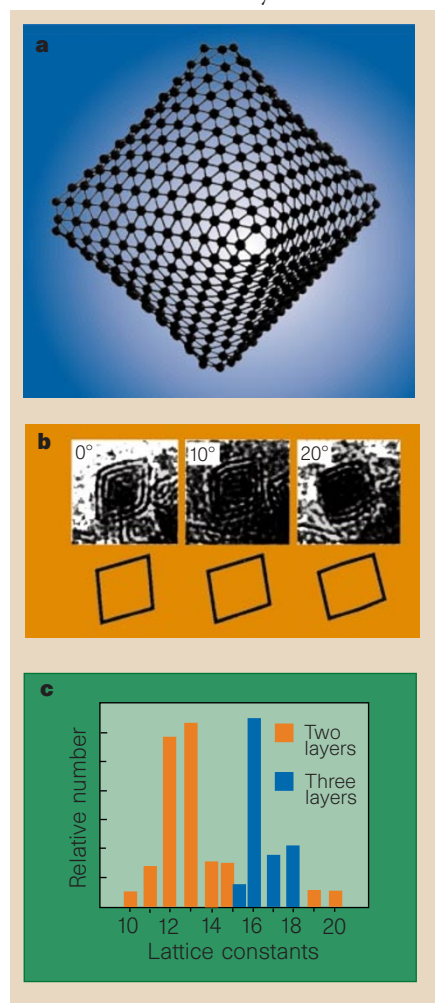


Figure 1 Structure of the molecules. **a**, Model octahedron with an edge length of 12 *a* lattice constants showing only the molybdenum sublattice. **b**, Transmission electron microscope images and model-generated projections for a three-layer MoS_2 rhomboid at 0° and undergoing tilts of 10° and 20°. **c**, Histogram of octahedral edge lengths in *a* lattice constants determined from 30 rhomboidal, rectangular and hexagonal projections observed by TEM.

1. Tenne, R., Margulis, L., Genut, M. & Hodes, G. *Nature* **360**, 444–446 (1992).
2. Chopra, N. G. *et al. Science* **269**, 966–967 (1995).
3. Tenne, R. *Adv. Mater.* **7**, 965–995 (1995).
4. Kroto, H. *Science* **242**, 1139–1145 (1988).
5. Kroto, H. W. *et al. Nature* **318**, 162–163 (1985).
6. Feldman, Y., Wasserman, E., Srolovitz, D. J. & Tenne, R. *Science* **267**, 222–225 (1995).
7. Wilson, J. A. & Yoffe, A. D. *Adv. Phys.* **18**, 193–335 (1969).